Theoretical and Applied Fracture Mechanics 90 (2017) 218–227

Contents lists available at ScienceDirect

Theoretical and Applied Fracture Mechanics

journal homepage: www.elsevier.com/locate/tafmec

# Relationship between strain rate concentration factor and stress concentration factor

Nao-Aki Noda *, Yunong Shen, Rei Takaki, Daichi Akagi, Tomohiro Ikeda, Yoshikazu Sano, Yasushi Takase

*Department of Mechanical Engineering, Kyushu Institute of Technology, 1-1 Sensui-cho, Tobata-ku, Kitakyushu-shi, Fukuoka 804-8550, Japan*

ARTICLE INFO

*Article history:*
Received 15 May 2017
Accepted 15 May 2017
Available online 25 May 2017

*Keywords:*
Notch fracture
High speed tensile test
Impact strength
Strain rate concentration factor
Stress concentration factor

ABSTRACT

In this study, the strain rate concentration is considered for high speed tensile test, which is now being recognized as a standard testing method. To evaluate the impact strength of engineering materials under high impact speed, Izod and Charpy tests are unsuitable since they cannot control the impact speeds and therefore do not coincide with the real failure of real products. For smooth specimens, the strain rate can be determined from the tensile speed $u/t$ and specimen length $l$ as $\dot{\varepsilon}_{smooth} = u/tl$. For notched specimens, however, the strain rate at the notch root $\dot{\varepsilon}_{notch}$ should be analyzed accurately. In this study, therefore, the strain rate concentration factor defined as $K_{t\dot{\varepsilon}} = \dot{\varepsilon}_{notch}/\dot{\varepsilon}_{smooth}$ is studied with varying the notch geometry and specimen length. It is found that the strain concentration factor $K_{t\dot{\varepsilon}}$ can be estimated from stress concentration factor $K_t^*$.



## 1. Introduction

Charpy and Izod tests are widely used to investigate the impact property of structural materials [1–4]. The strength of engineering materials varies depending on the temperature and high impact speed, especially known as the brittle–ductile transition behavior. Charpy impact test provides the absorbed energy under different temperature. However, the results are not closely related to the tensile properties such as tensile strength, yield strength and fatigue strength used in machine design. Moreover, Charpy impact speed does not correspond to the real failure of the real products. By considering those disadvantages, the high-speed tensile test is now being recognized as the standard impact strength test. Here, the tensile strength can be discussed through notched flat and round bar specimens under different tensile speed and temperature [5,6].

Previous studies suggested that the strain rate at the notch root may control the brittle–ductile transition behavior [7–12]. In the high speed tensile testing, it is therefore necessary to know the strain rate at the notch root accurately. Since it is almost impossible to measure the strain rate at the notch root experimentally, the strain rate concentration factor should be investigated analytically.

Previously the authors have proposed that the stress concentration factor formulas useful for arbitrary notch dimensions in notched specimens [16–21]. Regarding the strain rate concentration factor, however, the notch shape effects have not been clarified yet. In this paper, therefore, the strain rate concentration factor will be studied by varying the notch geometry. Then, the effects of notch root radius and notch depth on the strain rate concentration factor will be discussed. Finally, the relationship between the strain rate concentration factors and the previously studied stress concentration factors [16–21] will be clarified to evaluate the impact strength of engineering materials conveniently.

## 2. Definition of the strain rate concentration factor

Previously flat bar specimens are considered for evaluating the impact strength of polycarbonate. This study focuses on the round bar specimens in Fig. 1 since they are often used for metal testing. By considering JIS Z 2241 prescribing the test specimen, the specimen length $l = 40$ mm and the maximum specimen diameter $D = 8$ mm are mainly considered in this study. In addition, the notch opening angle is fixed as $\omega = 45°$.

Assume notch root radius $\rho = 0.25$ mm and $\rho = 2$ mm, while the notch depth varies from $t = 1$ mm to $t = 3.96$ mm. Here $\rho = 0.25$ mm corresponds to the notch root radius of the specimen in Charpy impact test. Also, here, to evaluate the strength of ductile cast iron, assume $\rho = 2$ mm, which corresponds to the sharpest notch root radius of casting products. Fig. 1(c) shows the FEM model for analysis in notch root radius $\rho = 0.25$ mm and the detail mesh of the notch root, while Fig. 1(d) shows the notch part correspond to $\rho = 2$ mm. The minimum mesh size at the notch root is

* Corresponding author.
*E-mail address:* noda@mech.kyutech.ac.jp (N.-A. Noda).

http://dx.doi.org/10.1016/j.tafmec.2017.05.017
0167-8442/

**Nomenclature**

| | |
|---|---|
| A | Material constant value = $10^8$ [$s^{-1}$] |
| $D$ | Maximum specimen diameter |
| $d$ | Minimum specimen diameter |
| $e$ | Minimum mesh size |
| $K_t$ | Net stress concentration factor |
| $K_t^*$ | Gross stress concentration factor = $K_t \cdot (D/d)^2$ |
| $K_{t\dot{\varepsilon}}$ | Strain rate concentration factor |
| $l$ | Specimen length |
| $l/D$ | Relative specimen length |
| $P$ | Applied load |
| $P_{max}$ | Maximum load obtained from the tensile test |
| R | Strain rate-temperature parameter |
| $u(t)$ | Displacement applied to the specimen end |
| $u(t)/t$ | Tensile speed assuming $u(t)$ is proportional to the time |
| T | Temperature |
| $t$ | Notch depth |
| $2t/D$ | Relative notch depth |
| $\dot{\varepsilon}_{max}$ | Maximum strain rate |
| $\dot{\varepsilon}_{nom}$ | Nominal strain rate |
| $\dot{\varepsilon}_{notch}$ | Strain rate in notched specimen |
| $\dot{\varepsilon}_{smooth}$ | Strain rate in smooth specimen |
| $\rho$ | Notch root radius |
| $2\rho/D$ | Relative notch radius |
| $\sigma_{Bnotch}$ | Tensile strength on the notch root |
| $\sigma_{gross}$ | Gross tensile stress = $4P/(\pi D^2) = \sigma_{net} \cdot (d/D)^2$ |
| $\sigma_{max}$ | Maximum stress |
| $\sigma_{net}$ | Net nominal stress = $4P/(\pi d^2) = \sigma_{net} \cdot (D/d)^2$ |
| $\omega$ | Notch opening angle = 45° |

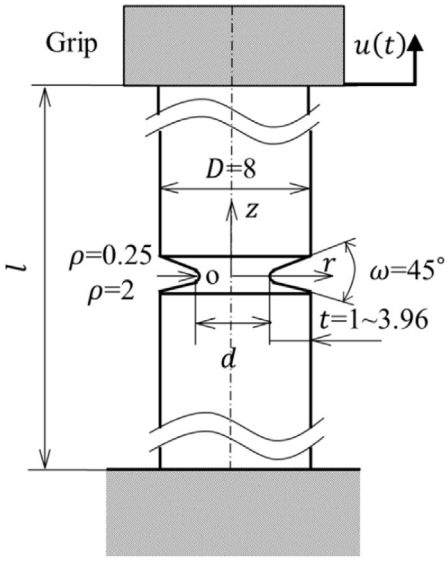


(a) Notched specimen (Dimensions : mm)

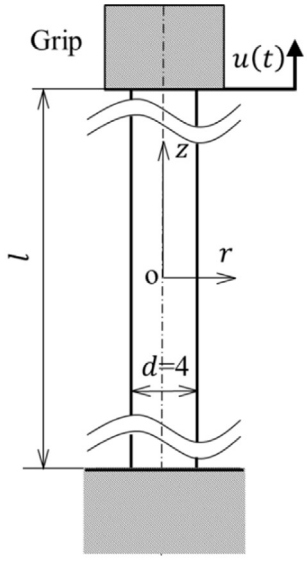


(b) Smooth specimen (Dimensions : mm)

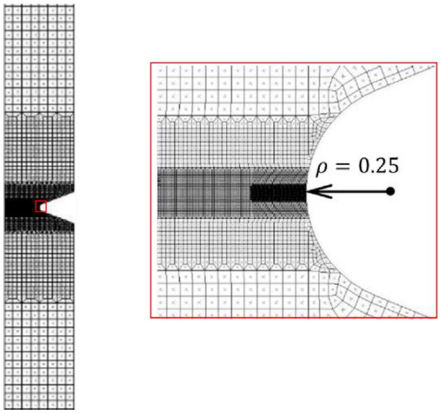


(c) FEM model and notch root detail ($\rho$=0.25mm)

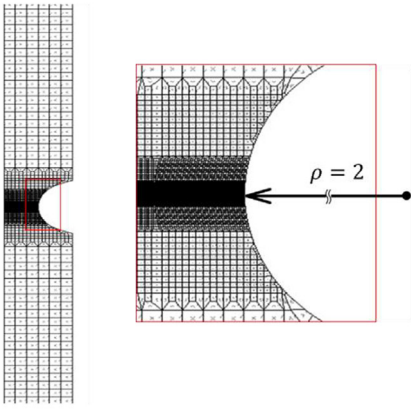


(d) FEM model and notch root detail ($\rho$=2mm)

**Fig. 1.** Geometry of specimens and FEM models (Dimensions: mm).

$e = \rho/243$. The static stress concentration factor obtained by the model of Fig. 2 coincide with the result in [7] within 1% error.

In the dynamic analysis, time step interval also affects the accuracy of the results. In this analysis, the time step $1 \times 10^6$ is found to

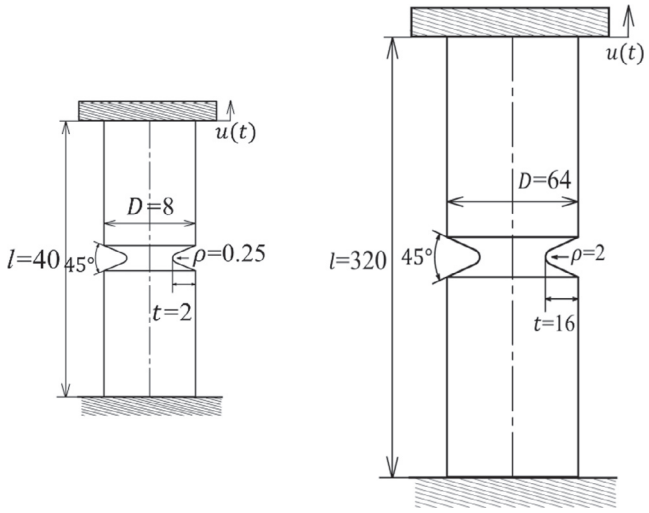


(a) Specimen 1 (b) Specimen 2 (8 times larger than specimen 1)

**Fig. 2.** Similar specimen (Dimension: mm).

be enough to obtain 3-digit-accuracy [22]. In a transient dynamic analysis, damping represents the dissipation of energy in the structural system. In FEM code MSC. Marc/Mentat 2011, the program bases integration on the usual assumption that the damping matrix of the system is a linear combination of the mass and stiffness matrices. Element damping uses coefficients on the element matrices and is represented by the equation

$$[C] = \alpha[M] + \beta[K] \tag{1}$$

Here, [C] is the global damping matrix, [M] is the mass matrix and [K] is the stiffness matrix.

Because of the same damping coefficients are used throughout the structure, the following equation can be used to obtain the mass damping coefficient $\alpha$ and the usual stiffness damping coefficient $\beta$. The mass damping coefficient and the usual stiffness damping coefficient will be used for the dynamic analysis.

$$\zeta = \frac{1}{2}\left(\frac{\alpha}{\omega} + \beta\omega\right) \tag{2}$$

Here, $\zeta$ is the damping ratio, and $\omega$ is the frequency which can be calculated by FEM.

As shown in Appendix A, the strain rates in notched and smooth specimens $\dot{\varepsilon}_{notch}, \dot{\varepsilon}_{smooth}$ increase with increasing the tensile speed. However, the ratio $K_{t\dot{\varepsilon}} = \dot{\varepsilon}_{notch}/\dot{\varepsilon}_{smooth}$ is always constant independent of the tensile speed.

Since the strain rate in smooth specimen is expressed in Eq. (3), the strain rate at the notch root can be obtained from the tensile speed $u(t)/t$ and the strain rate concentration factor $K_{t\dot{\varepsilon}}$. Here, $u(t)$ is the displacement applied to the specimen end, which is assumed to be proportional to the time $t$.

$$\dot{\varepsilon}_{smooth} = \frac{u(t)/l}{t} \tag{3}$$

$$K_{t\dot{\varepsilon}} = \frac{\dot{\varepsilon}_{notch}}{\dot{\varepsilon}_{smooth}}, \quad \dot{\varepsilon}_{notch} = K_{t\dot{\varepsilon}} \cdot \dot{\varepsilon}_{smooth} = K_{t\dot{\varepsilon}} \cdot \frac{u(t)/l}{t} \tag{4}$$

## 3. Strain rate concentration factor for similar geometry

First, as shown in Fig. 2, the strain rate concentration factors in similar test specimen geometries were investigated. The results are shown in Table 1. As can be seen from Table 1, similar to the stress concentration factor, the strain rate concentration factor is found to be the same for similar specimens. From Table 1, it may be concluded that the strain rate concentration factor depends on the geometry of the specimens, but independent of the specimen size.

**Table 1**
Similarity of strain rate concentration factor $K_{t\dot{\varepsilon}}$ in Fig. 2.

| | Specimen 1 | Specimen 2 |
|---|---|---|
| $\dot{\varepsilon}_{notch}$ | 0.215 [$s^{-1}$] | 1.726 [$s^{-1}$] |
| $\dot{\varepsilon}_{smooth}$ | 0.0313 [$s^{-1}$] | 0.250 [$s^{-1}$] |
| $K_{t\dot{\varepsilon}} = \frac{\dot{\varepsilon}_{notch}}{\dot{\varepsilon}_{smooth}}$ | 6.896 | 6.902 |

## 4. Effect of specimen length on the strain rate concentration factor

It is known that the net stress concentration factor $K_t$ is independent of the specimen length $l$ if $l/D \geqq 1$ in Fig. 1(a). However, different from the net stress concentration factor $K_t$, the strain rate concentration factor $K_{t\dot{\varepsilon}}$ is depending on the specimen length $l/D$ (see Appendix A).

Under fixed maximum specimen diameter $D$ = 8 mm, the strain rate concentration factor $K_{t\dot{\varepsilon}}$ is calculated by varying the specimen length $l$. Table 2 shows the results for the relative notch radius $2\rho/D$ = 0.0625, $2\rho/D$ = 0.5 and the relative notch depth $2t/D$ = 0.25, $2t/D$ = 0.5 by varying the relative specimen length $l/D$ = 1–2560. As can be seen from Table 2, the notch depth $t$ is put as $t$ = 0.0625, 0.25, 1, 2 mm while the notch root radius $\rho$ is put as $\rho$ = 0.25, 2 mm. The column in Table 2 indicates the region where the $K_{t\dot{\varepsilon}}$ difference is less than 1%. The JIS specimen dimensions $l$ = 40, $D$ = 8, $l/D$ = 5 prescribed by JIS Z 2241 will be discussed in Section 5, so the results are underlined.

Table 3 shows the net stress concentration factor $K_t$ and the gross stress concentration factor $K_t^* = K_t \cdot (D/d)^2$ under different specimen length. The net stress concentration factor $K_t$ is usually defined as $K_t = \sigma_{max}/\sigma_{net}$ as shown in Eq. (5) based on the net nominal stress $\sigma_{net} = 4P/\pi d^2$. The gross stress concentration factor $K_t^*$ is defined as shown in Eq. (6) based on the gross tensile stress $\sigma_{gross} = 4P/\pi D^2$.

$$K_t = \frac{\sigma_{max}}{\sigma_{net}} \tag{5}$$

$$K_t^* = \frac{\sigma_{max}}{\sigma_{gross}} = K_t \cdot \left(\frac{D}{d}\right)^2, \quad \sigma_{gross} = \sigma_{net} \cdot \left(\frac{d}{D}\right)^2 \tag{6}$$

Fig. 3 compares the strain rate concentration factor $K_{t\dot{\varepsilon}}$ and the gross stress concentration factor $K_t^*$ by varying the relative specimen length $l/D$. In Fig. 3, it is seen the results for $2\rho/D$ = 0.0625 is always larger than the results for $2\rho/D$ = 0.5 and varies depending on $2t/D$ similar to the gross stress concentration factor $K_t^*$. Although the gross stress concentration factor $K_t^*$ is constant independent of the specimen length, the strain rate concentration factor $K_{t\dot{\varepsilon}}$ increases with the increasing specimen length $l$, and becomes constant if $l$ is large enough.

## 5. Relationship between the strain rate concentration factor and the stress concentration factor

By considering JIS Z 2241 prescribing the tensile test specimen in Fig. 4, the specimen length $l$ = 40 mm and the diameter $D$ = 8 mm are assumed in this chapter. The results of the strain rate concentration factor $K_{t\dot{\varepsilon}}$ are shown in Table 4 and Fig. 5 by varying the relative notch depth $2t/D$ for fixed relative notch radius $2\rho/D$ = 0.0625 and $2\rho/D$ = 0.5. Here, $2\rho/D$ = 0.0625 corresponds to the notch radius $\rho$ = 0.25 mm of the specimen used in the Charpy

**Table 2**
Strain rate concentration factor $K_{t\dot{\varepsilon}}$ under different length and $D$ = 8 mm in Fig. 1(a). ☐:less than 1% difference.

| $K_{t\dot{\varepsilon}}$ | | | | | | | | | |
|---|---|---|---|---|---|---|---|---|---|
| | | $t$=0.0625mm ($2t/D$=0.015625) | | $t$=0. 25mm ($2t/D$=0.0625) | | $t$=1mm ($2t/D$=0.25) | | $t$=2mm ($2t/D$=0.5) | |
| $l/D$ | $l$(mm) | $\rho$ =0.25mm ($2\rho/D$=0.0625) | $\rho$ =2mm ($2\rho/D$=0.25) | $\rho$ =0.25mm ($2\rho/D$=0.0625) | $\rho$ =2mm ($2\rho/D$=0.25) | $\rho$ =0.25mm ($2\rho/D$=0.0625) | $\rho$ =2mm ($2\rho/D$=0.25) | $\rho$ =0.25mm ($2\rho/D$=0.0625) | $\rho$ =2mm ($2\rho/D$=0.25) |
| 1.00 | 8 | 1.894 | 1.286 | 2.900 | 1.602 | 4.969 | 2.058 | 5.580 | 2.237 |
| 1.25 | 10 | 1.920 | 1.303 | 2.940 | 1.627 | 4.902 | 2.163 | 6.128 | 2.490 |
| 1.5 | 12 | 1.933 | 1.313 | 2.963 | 1.642 | 5.046 | 2.240 | 6.629 | 2.718 |
| 1.75 | 14 | 1.940 | 1.316 | 2.976 | 1.649 | 5.270 | 2.297 | 7.049 | 2.916 |
| 2 | 16 | 1.941 | 1.317 | 2.982 | 1.654 | 5.232 | 2.344 | 7.405 | 3.090 |
| 2.5 | 20 | 1.938 | 1.316 | 2.985 | 1.656 | 5.344 | 2.410 | 8.055 | 3.374 |
| 3.5 | 28 | 1.933 | 1.312 | 2.983 | 1.657 | 5.474 | 2.489 | 8.836 | 3.775 |
| 5(JIS) | 40 | 1.929 | 1.310 | 2.980 | 1.658 | 5.576 | 2.553 | 9.528 | 4.148 |
| 10 | 80 | 1.925 | 1.308 | 2.980 | 1.659 | 5.700 | 2.633 | 10.488 | 4.685 |
| 40 | 320 | 1.923 | 1.306 | 2.980 | 1.660 | 5.798 | 2.693 | 11.236 | 5.190 |
| 80 | 640 | 1.922 | 1.305 | 2.979 | 1.660 | 5.814 | 2.705 | 11.391 | 5.285 |
| 160 | 1280 | 1.921 | 1.305 | 2.979 | 1.660 | 5.824 | 2.710 | 11.584 | 5.333 |
| 320 | 2560 | 1.921 | 1.305 | 2.978 | 1.660 | 5.824 | 2.712 | 11.622 | 5.358 |
| 640 | 5120 | 1.921 | 1.305 | 2.978 | 1.660 | 5.828 | 2.713 | 11.643 | 5.371 |
| 1280 | 10240 | 1.921 | 1.305 | 2.978 | 1.660 | 5.829 | 2.714 | 11.653 | 5.376 |
| 2560 | 20480 | 1.921 | 1.305 | 2.978 | 1.660 | 5.830 | 2.714 | 11.653 | 5.379 |

**Table 3**
Stress concentration factor under different length ($D$ = 8 [mm] in Fig. 1(a)).

| $l/D$ | $l$ [mm] | $t$ = 0.0625 [mm] ($2t/D$ = 0.0156) | | $t$ = 0. 25 [mm] ($2t/D$ = 0.0625) | | $t$ = 1 [mm] ($2t/D$ = 0.25) | | $t$ = 2 [mm] ($2t/D$ = 0.5) | |
|---|---|---|---|---|---|---|---|---|---|
| | | $\rho$ = 0.25 [mm] ($2\rho/D$ = 0.0625) | $\rho$ = 2 [mm] ($2\rho/D$ = 0.25) | $\rho$ = 0.25 [mm] ($2\rho/D$ = 0.0625) | $\rho$ = 2 [mm] ($2\rho/D$ = 0.25) | $\rho$ = 0.25 [mm] ($2\rho/D$ = 0.0625) | $\rho$ = 2 [mm] ($2\rho/D$ = 0.25) | $\rho$ = 0.25 [mm] ($2\rho/D$ = 0.0625) | $\rho$ = 2 [mm] ($2\rho/D$ = 0.25) |
| $K_t$ | | | | | | | | | |
| all | | 1.944 | 1.295 | 2.697 | 1.518 | 3.553 | 1.615 | 3.185 | 1.420 |
| $K_t^* = K_t \cdot (D/d)^2$ | | | | | | | | | |
| all | | 2.006 | 1.336 | 3.069 | 1.727 | 6.316 | 2.871 | 12.740 | 5.680 |
| $K_{t\dot{\varepsilon}}/K_t$ | | | | | | | | | |
| 5 | 40 | 0.992 | 1.012 | 1.105 | 1.092 | 1.569 | 1.581 | 2.992 | 2.921 |
| $K_{t\dot{\varepsilon}}/K_t^*$ | | | | | | | | | |
| 5 | 40 | 0.962 | 0.980 | 0.971 | 0.960 | 0.883 | 0.889 | 0.748 | 0.730 |

impact test. Also, $\rho$ = 2 mm with $D$ = 8 mm corresponds to the sharpest case of the notch root radius when high Si ductile cast iron is used as structural components [9]. As shown in Fig. 5(a), the strain rate concentration factor increases with increasing the relative notch depth. The same results are also indicated in Table 4 and Fig. 5(b).

The stress concentration factor of notched specimen is usually defined as $K_t = \sigma_{max}/\sigma_{net}$ based on the net nominal stress $\sigma_{net} = 4P/\pi d^2$. Since $\sigma_{net} \to \infty$ as $2t/D \to 1$, $K_t \to 1$ as $2t/D \to 1$. Under a fixed value of $2\rho/D$, the results of $2t/D$ = 0 correspond to the smooth specimen without notch.

Fig. 6 shows the ratio $K_{t\dot{\varepsilon}}/K_t$ vs. $2t/D$. When the relative notch depth $2t/D \to 1$, the ratio $K_{t\dot{\varepsilon}}/K_t \to \infty$. Here, the net stress concentration factor $K_t$ is defined as Eq. (5) from the maximum stress $\sigma_{max}$ and the net nominal stress $\sigma_{net}$ at the minimum cross section. When the relative notch depth $2t/D \to 1$, the strain rate concentration factor $K_{t\dot{\varepsilon}} \to \infty$ but the net stress concentration factor $K_t \to 1$. Therefore, the gross stress concentration factor $K_t^*$ is defined as Eq. (6) from the maximum stress $\sigma_{max}$ and the gross tensile stress $\sigma_{gross}$. When the relative notch depth $2t/D \to 1$, the strain rate concentration factor $K_t^* \to \infty$. When the relative notch depth $2t/D \leqslant 0.5$, the strain rate concentration factor $K_{t\dot{\varepsilon}}$ and the net stress concentration factor $K_t$ are nearly the same.

Then, the relationship between the strain rate concentration factor $K_{t\dot{\varepsilon}}$ and the gross stress concentration factor $K_t^*$ is investigated.

Table 5 and Fig. 7 show the relationship between the ratio $K_{t\dot{\varepsilon}}/K_t^*$ and the relative notch depth $2t/D$. It is found that the value

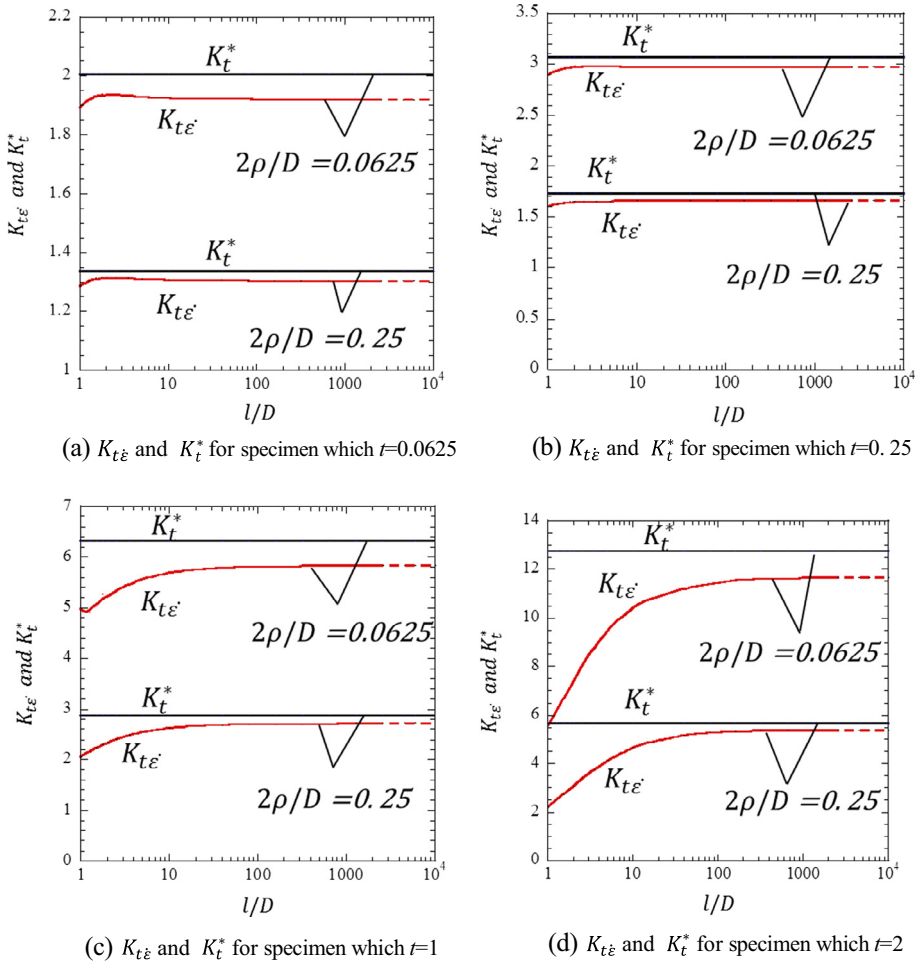


(a) $K_{t\dot{\varepsilon}}$ and $K_t^*$ for specimen which $t$=0.0625

(b) $K_{t\dot{\varepsilon}}$ and $K_t^*$ for specimen which $t$=0. 25

(c) $K_{t\dot{\varepsilon}}$ and $K_t^*$ for specimen which $t$=1

(d) $K_{t\dot{\varepsilon}}$ and $K_t^*$ for specimen which $t$=2

**Fig. 3.** Strain rate concentration factor $K_{t\dot{\varepsilon}}$ and gross stress concentration factor $K_t^*$ ($K_t^* = K_t \cdot D^2/d^2$) under different length in Fig. 1(a).

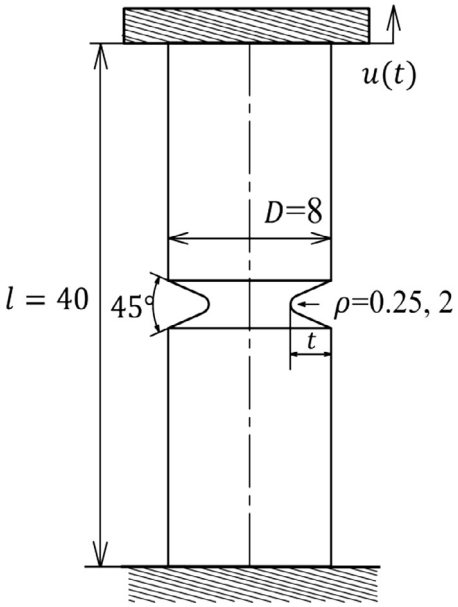


**Fig. 4.** Notch specimens considered based on JIS Z 2241.

of $K_{t\dot{\varepsilon}}/K_t^*$ is almost the same for $2\rho/D = 0.0625$ and $2\rho/D = 0.5$ when the relative notch depth $2t/D \leqslant 0.5$. From Fig. 7, it is found that the value of $K_{t\dot{\varepsilon}}/K_t^*$ is insensitive to the notch root radius in the range of $2t/D \leqslant 0.5$. By using this fact, the strain rate concentration factor $K_{t\dot{\varepsilon}}$ can be estimated from the gross stress concentration factor $K_t^*$.

## 6. Usefulness of the strain rate concentration factor

High Si ductile cast iron is now being considered to be used as structural components in several industrial fields [23,24]. Table 6 shows the mechanical properties of the high Si ductile cast iron. By taking this as an example, the usefulness will be shown for the strain rate concentration factor [9]. Consider the specimen in Fig. 4 with the specimen length $l = 40$ mm, the diameter $D = 8$ mm, the notch opening angle $\omega = 45°$, the notch root radius $\rho = 0.25$ mm and the notch depth $t = 2$ mm. Then, tensile test is conducted by varying the temperature and tensile speed. Fig. 8 shows the strain rate $\dot{\varepsilon}_{notch}$, $\dot{\varepsilon}_{smooth}$ in both notched and smooth specimens as well as the strain rate concentration factor $K_{t\dot{\varepsilon}}$. As shown in Fig. 8, the strain rate of the notch root can be obtained for an arbitrary tensile speed $u(t)/t$ by using Eq. (2) with $K_{t\dot{\varepsilon}} = 9.49$.

Table 7 shows the tensile strength on the notch root $\sigma_{Bnotch} = 4P/\pi d^2$ at the temperature $T = 25$ °C under different tensile speed $u(t)/t$. Here, $P_{max}$ is the maximum load obtained from the tensile test. Fig. 9 shows the relationship between the strain rate in notched specimen $\dot{\varepsilon}_{notch}$ and the tensile strength on the notch root $\sigma_{Bnotch}$ under constant temperature $T = 25$ °C. Fig. 9 shows that the tensile strength slightly increases with increasing the strain rate and after taking a peek value starts decreasing around $\dot{\varepsilon}_{notch} = 3.3$ [s$^{-1}$].

**Table 4**
Strain rate concentration factor and the net stress concentration factor when $l/D = 5$ ($l = 40$ mm, $D = 8$ mm).

| $2t/D$ | $K_{t\dot{\varepsilon}}$ | | | $K_t$ | | |
|---|---|---|---|---|---|---|
| | $2\rho/D = 0.0625$ | $2\rho/D = 0.1$ | $2\rho/D = 0.5$ | $2\rho/D = 0.0625$ | $2\rho/D = 0.1$ | $2\rho/D = 0.5$ |
| 0.00 | 1.000 | 1.000 | 1.000 | 1.000 | 1.000 | 1.000 |
| 0.25 | 5.581 | 4.578 | 2.554 | 3.550 | 2.914 | 1.619 |
| 0.50 | 9.490 | 7.732 | 4.145 | 3.185 | 2.590 | 1.420 |
| 0.75 | 18.500 | 15.040 | 8.334 | 2.334 | 1.901 | 1.204 |
| 0.90 | 38.000 | 31.488 | 17.190 | 1.610 | 1.393 | 1.086 |
| 0.99 | 167.000 | 136.712 | 63.060 | 1.070 | 1.045 | 1.008 |
| →1.00 | →∞ | →∞ | →∞ | →1.000 | →1.000 | →1.000 |

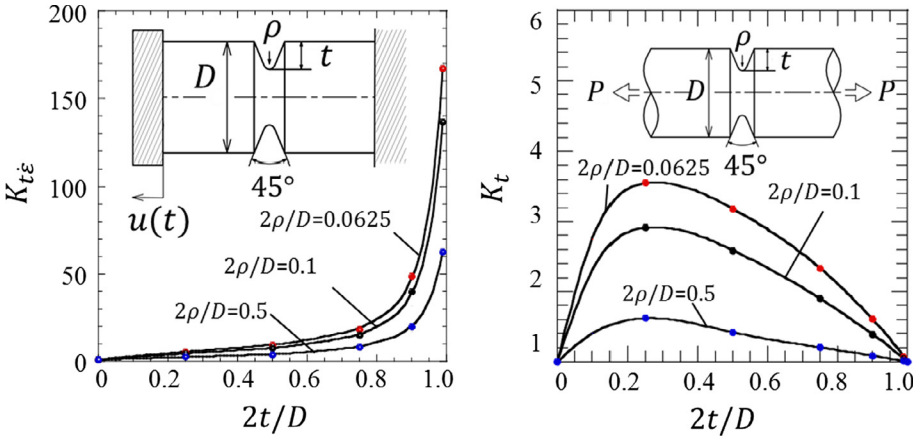


(a) Relationship between $K_{t\dot{\varepsilon}}$ and $2t/D$ when $l/D=5$ ($l$=40mm, $D$=8mm)

(b) Relationship between $K_t$ and $2t/D$ when $l/D=5$ ($l$=40mm, $D$=8mm)

**Fig. 5.** $K_{t\dot{\varepsilon}}$ vs. $2t/D$ and $K_t$ vs. $2t/D$ when $l/D = 5$ ($l = 40$ mm, $D = 8$ mm).

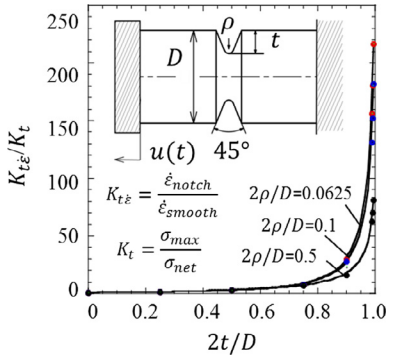


**Fig. 6.** Relationship between $K_{t\dot{\varepsilon}}/K_t$ and $2t/D$ when $l/D = 5$ ($l = 40$ mm, $D = 8$ mm).

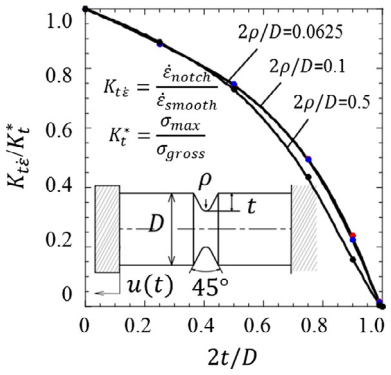


**Fig. 7.** Relationship between $K_{t\dot{\varepsilon}}/K_t^*$ and $2t/D$ when $l/D = 5$ ($l = 40$ mm, $D = 8$ mm).

On the other hand, Fig. 10 shows the tensile strength under constant strain rate in notched specimen by varying the temperature. As can be seen from Fig. 10, the tensile strength starts decreasing around $T = -25$ °C with decreasing the temperature.

Next, in order to evaluate both effects of strain rate and temperature in a similar way, the tensile strength on the notch root $\sigma_{Bnotch}$ is plotted by using the strain rate-temperature parameter R which is expressed in Eq. (7).

**Table 5**
Ratio of strain rate concentration factor and stress concentration factor when $l/D = 5$ ($l = 40$ mm, $D = 8$ mm).

| $2t/D$ | $K_{t\dot{\varepsilon}}/K_t$ | | | $K_{t\dot{\varepsilon}}/K_t^*$ | | |
|---|---|---|---|---|---|---|
| | $2\rho/D = 0.0625$ | $2\rho/D = 0.1$ | $2\rho/D = 0.5$ | $2\rho/D = 0.0625$ | $2\rho/D = 0.1$ | $2\rho/D = 0.5$ |
| 0.00 | 1.000 | 1.000 | 1.000 | 1.000 | 1.000 | 1.000 |
| 0.25 | 1.572 | 1.572 | 1.574 | 0.884 | 0.884 | 0.889 |
| 0.50 | 2.979 | 2.984 | 2.923 | 0.745 | 0.746 | 0.730 |
| 0.75 | 7.940 | 7.920 | 6.958 | 0.498 | 0.495 | 0.435 |
| 0.90 | 23.600 | 22.600 | 15.770 | 0.238 | 0.226 | 0.158 |
| 0.99 | 156.100 | 131.000 | 62.440 | 0.0156 | 0.0131 | 0.00627 |
| →1.00 | →∞ | →∞ | →∞ | →0.000 | →0.000 | →0.000 |

**Table 6**
Mechanical properties implemented in accordance with JIS Z 2241.

| Material | Tensile strength $\sigma_B$ [MPa] | 0.2% proof stress $\sigma_b$ [MPa] | Stiffness $E$ [GPa] | Fracture strain $\varepsilon_b$ [%] |
|---|---|---|---|---|
| SSFDI500 | 525 | 401 | 172 | 21 |

**Table 7**
Results of high speed tensile test of high Si ductile cast iron obtained by using Fig. 4 ($T$ = 25 °C).

| Tensile speed $u(t)/t$ [mm/s] | Strain rate at the notch root $\dot{\varepsilon}_{notch}$ [$s^{-1}$] | Tensile strength $\sigma_{Bnotch}$ [MPa] |
|---|---|---|
| 0.0100 | 0.0024 | 762 |
| 0.8400 | 0.1993 | 836 |
| 18.1000 | 4.2942 | 876 |

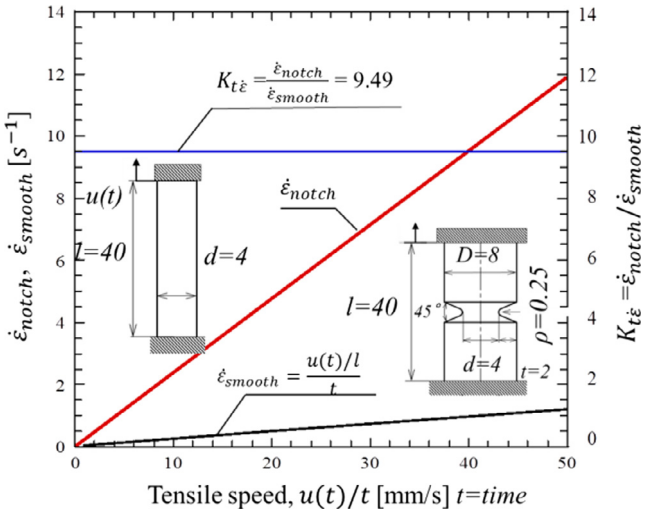


**Fig. 8.** $K_{t\dot{\varepsilon}}$ vs. tensile speed for Fig. 1(a) and (b).

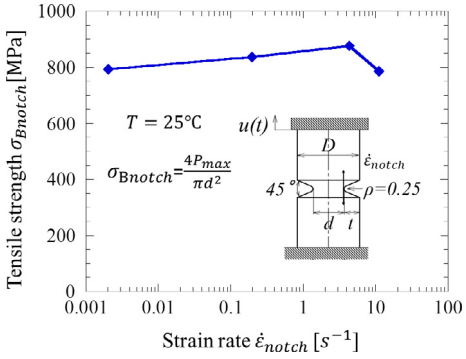


**Fig. 9.** Relationship between $\sigma_{Bnotch}$ and $\dot{\varepsilon}_{notch}$.

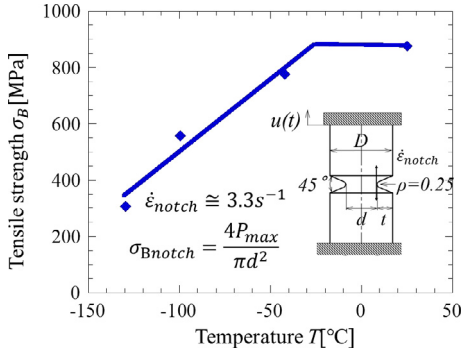


**Fig. 10.** Relationship between $\sigma_{Bnotch}$ and $T$.

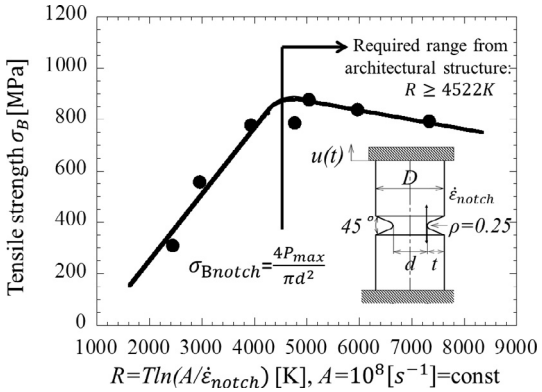


**Fig. 11.** Relationship between $\sigma_{Bnotch}$ and R-value.

$$R = T \ln\left(\frac{A}{\dot{\varepsilon}_{notch}}\right) \tag{7}$$

Here, $T$ = temperature [°C], A = $10^8$ [$s^{-1}$] and $\dot{\varepsilon}_{notch}$ is the strain rate in notched specimen [7,12]. The strain rate-temperature parameter R in Eq. (7) has been introduced to explain the influence of $\dot{\varepsilon}_{notch}$ and $T$ on the tensile strength as well as yield stress of steel [7–15]. Bennett et al. showed that the strain rate and temperature effects on the yield stress can be expressed by the R value for steel and BCC metals [7] and then Fujii et al. has experimentally supported as well [8,13].

By using R parameter (7), the results in Figs. 9 and 10 can be expressed as a unique master curve as shown in Fig. 11. From Fig. 11, it can be seen that the tensile strength increases with the decreasing R, but starts decreasing around R = 5000. The master curve expresses the brittle–ductile transition behavior uniquely in the strain rate range of $10^{-3}$–10 [$s^{-1}$] and in the temperature range of −130 to 25 [°C]. As shown in Fig. 8, the strain rate in notched specimen is 9.49 times larger than strain rate in smooth specimen. This may reduce the R value by about 600, which is equivalent to reducing the temperature by about 35 °C. As shown in Fig. 11, high Si ductile cast iron shows brittle-ductile transition at R ≅ 4500, which is larger than that of a conventional ductile cast iron FCD500 (R ≅ 2500). However, it should be noted that the tensile strength on the notch root $\sigma_{Bnotch}$ is still large enough in the range of R parameter required for architectural structure R ≥ 4522 [25,26]. Therefore, when we use high Si ductile cast iron, tensile strength $\sigma_{Bnotch}$ can be larger enough for structural design of architectural components.

## 7. Conclusion

In this paper, the strain rate concentration at the notch root is considered in the high speed tensile test which is now replacing Charpy impact test. In particular, the relationship between the strain rate concentration factor and the stress concentration factor was investigated by varying the notch geometry and specimen length. After summarizing the results in Tables and Figures, the following conclusions were obtained.

(1) The strain rate concentration factor $K_{t\dot{\varepsilon}}$ was defined as the ratio of the strain rate in notched specimen to the strain rate in smooth specimen. Then, the maximum strain rate $\dot{\varepsilon}$ at the notch root can be obtained easily from the strain rate concentration factor.
(2) Similar to the stress concentration factor $K_t$, the strain rate concentration factor $K_{t\dot{\varepsilon}}$ has the same value if the specimen geometries are similar.
(3) Different from the stress concentration factor $K_t$ independent of the specimen length, the strain rate concentration factor $K_{t\dot{\varepsilon}}$ increases with increasing the specimen length and then become constant as shown in Fig. 3.
(4) It is found that the value of $K_{t\dot{\varepsilon}}/K_t^*$ is almost the same independent of the notch root radius when the relative notch depth $2t/D \leqq 0.5$. By using this relationship, the strain rate concentration factor $K_{t\dot{\varepsilon}}$ can be determined from the gross stress concentration factor $K_t^*$.

## Acknowledgement

The authors wish to express our thanks to the member of our group Ms. Akane Inoue for preparing the data and supporting FEM analysis.

## Appendix A. Results for notched flat bar specimen in high speed tensile test

In the previous study, the impact strength of polycarbonate was considered by using notched flat bar varying the tensile speed and temperature in high speed tensile test [5,6]. Then, the time-temperature independent principle was found for the fracture strain in terms of the strain rate at the notch root. It was seen that the obtained master curve was useful for predicting the ductility/brittle fracture for the wide range of strain rate and temperature. In this study, the strain rate distribution was considered at the

**Table A.1**
Mechanical properties implemented in accordance with JIS K 7161 and 7162.

| Material | Yield stress $\sigma_y$ [MPa] | Stress at break $\sigma_b$ [MPa] | Stiffness $E$ [GPa] | Nominal strain at Break $\varepsilon_b$ [%] (Gauge length = 115 mm) |
|---|---|---|---|---|
| PC | 62 | 73 | 2.3 | 111 |

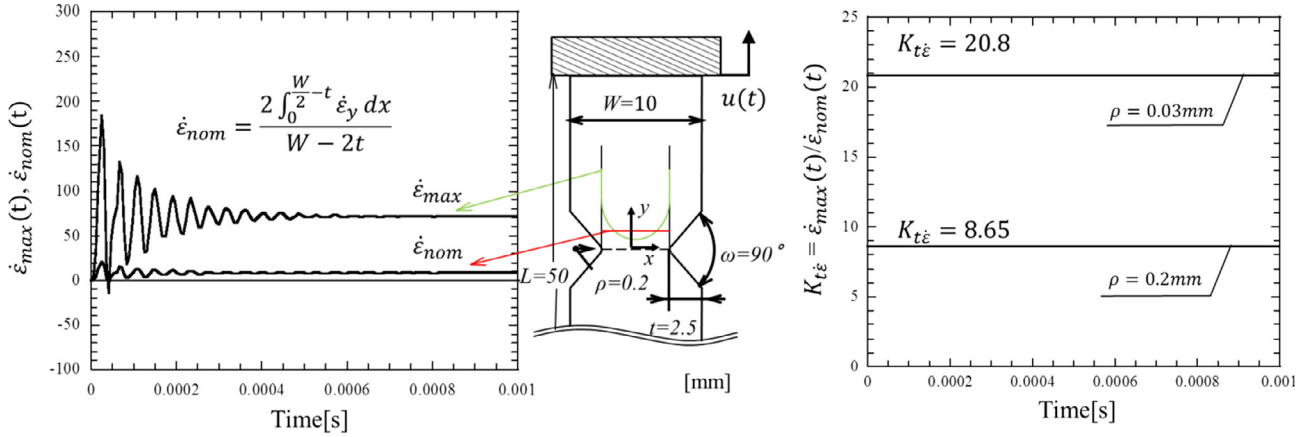


(a) Maximum strain rate and nominal strain rate (b) Strain rate concentration factor

**Fig. A.1.** Constancy of strain rate concentration factor (Plate specimen).

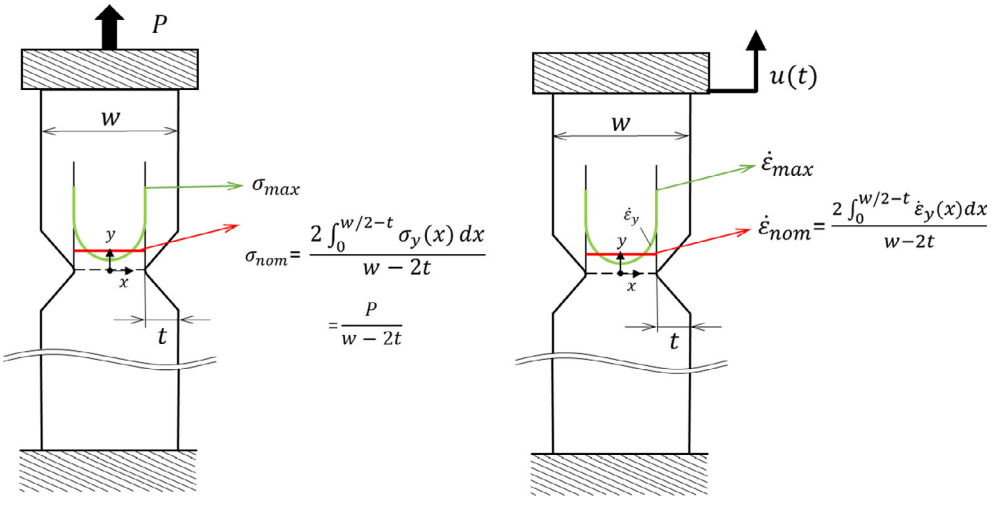


(a) $K_t = \sigma_{max}/\sigma_{nom}$ (b) $K_{t\dot{\varepsilon}} = \dot{\varepsilon}_{max}/\dot{\varepsilon}_{nom}$

**Fig. A.2.** Nominal stress $\sigma_{nom}$ and nominal strain rate $\dot{\varepsilon}_{nom}$ (Plate specimen).

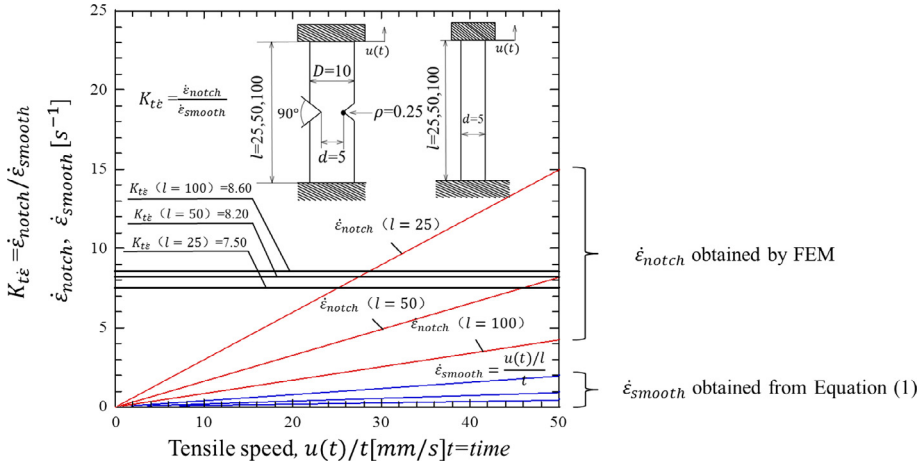


**Fig. A.3.** $K_{t\dot{\varepsilon}} = \dot{\varepsilon}_{notch}/\dot{\varepsilon}_{smooth}$ vs. tensile speed for different specimen length $l$.

minimum cross section of the specimen similar to the stress concentration factor. In this case, it is necessary to calculate the nominal strain rate $\dot{\varepsilon}_{nom}$ at the minimum section from the strain rate distribution when the maximum strain rate $\dot{\varepsilon}_{max}$ occurs at the notch root. Then, the strain rate concentration factor $K_{t\dot{\varepsilon}} = \dot{\varepsilon}_{max}/\dot{\varepsilon}_{nom}$ is calculated [6].

Table A.1 shows mechanical properties of polycarbonate. Fig. A.1(a) shows the strain rate $\dot{\varepsilon}_{max}(t)$ at the notch root at the time t as well as the nominal strain rate $\dot{\varepsilon}_{nom}(t)$ obtained from the strain rate distribution. Fig. A.1 (b) show $K_{t\dot{\varepsilon}}$ (= $\dot{\varepsilon}_{max}/\dot{\varepsilon}_{nom}$) obtained from $\dot{\varepsilon}_{max}$ and $\dot{\varepsilon}_{nom}$. Those results are obtained from the flat notched specimen with the specimen length $l$ = 50 mm, the width $W$ = 10 mm, the notch root radius $\rho$ = 0.2 mm, the notch depth $t$ = 2.5 mm and the notch opening angle $\omega$ = 90°. Fig. A.1 (b) shows $K_{t\dot{\varepsilon}}(t)$ at each time $t$. Here, $K_{t\dot{\varepsilon}}(t)$ = 20.8 is distinct for $\rho$ = 0.03 mm and $K_{t\dot{\varepsilon}}(t)$ = 8.65 is distinct for $\rho$ = 0.2 mm It is seen that $K_{t\dot{\varepsilon}}(t)$ is always constant independent of the time.

In the previous study, the strain rate concentration factor was defined as $K_{t\dot{\varepsilon}} = \dot{\varepsilon}_{max}/\dot{\varepsilon}_{nom}$. This definition has the following problem. Even if the strain rate concentration factor $K_{t\dot{\varepsilon}}$ is known for the specimen geometry used in experiments, the nominal strain rate $\dot{\varepsilon}_{nom}$ at the minimum section is necessary to obtain the maximum strain rate at the notch root $\dot{\varepsilon}_{max}$. Since the strain rate distribution of the minimum section varies depending on the notch shape, it is not very easy to calculate $\dot{\varepsilon}_{nom}$. Regarding the stress concentration factor, the nominal stress $\sigma_{nom}$ in Fig. A.2(a) can be easily obtained from the applied load. However, the nominal strain rate $\dot{\varepsilon}_{nom}$ in Fig. A.2(b) has to be calculated by integrating the distribution to obtain the average value. In this paper, therefore, instead of the strain rate distribution at the minimum cross section, the strain rate generated in the smooth specimen is considered as a reference value. In other words, instead of $\dot{\varepsilon}_{max}/\dot{\varepsilon}_{nom}$, the strain rate concentration factor is newly defined as $\dot{\varepsilon}_{notch}/\dot{\varepsilon}_{smooth}$, the ratio of the maximum strain rate of the notched specimen to the strain rate of the smooth specimen.

Fig. A.3 shows the relationship between the strain rate of the smoothing material for the specimen length $l$ = 25, 50, 100 mm and the tensile speed. As shown in Fig. A.3, the strain rate of the smooth specimen increases proportionally to the tensile speed as shown in Eq. (3). Here, $u(t)/t$ is the tensile speed assuming $u(t)$ is proportional to the time, and $t$ is the time. Fig. A.3 also shows the strain rates for the notched and smooth specimens $\dot{\varepsilon}_{notch}$, $\dot{\varepsilon}_{smooth}$ and the strain rate concentration factor $K_{t\dot{\varepsilon}}$ defined as Eqs. (3) and (4). Here, the geometry of the notched and smooth specimens are indicated in Fig. A.1. Here, the notched flat specimen has a notch root radius $\rho$ = 0.2 mm.

As shown in Fig. A.1, since the strain rates for the notched and smooth specimens increase in proportion to the tensile speed, the ratio $K_{t\dot{\varepsilon}}$ does not depend on the tensile speed and is always constant. Therefore, if the strain rate concentration factor $K_{t\dot{\varepsilon}}$ is known, which is defined as the ratio of the notched specimen to the smooth specimen as shown in Eq. (4), the strain rate at the notch root can be obtained from the tensile speed $u(t)/t$ and the strain rate concentration factor $K_{t\dot{\varepsilon}}$.

Note that as shown in Fig. A.3 the strain rate concentration factor $K_{t\dot{\varepsilon}}$ is depending on the specimen length $l/D$ on the contrary to the net stress concentration factor $K_t$.

## References

[1] G. Roebben, A. Lamberty, J. Pauwels, Certification of Charpy V-notch reference test pieces at IRMM, in: Pendul. Impact Mach. Proced. Specimens, 2006, pp. 40–48.
[2] S. Kenji, J. Masaki, Physical interpretation for the upper shelf energy of weld zone in Charpy impact test, Trans. Jpn. Weld. Soc. 14 (1983) 61 (in Japanese).
[3] B. Tanguy, J. Besson, R. Piques, A. Pineau, Ductile to brittle transition of an A508 steel characterized by Charpy impact test. Part II: Modeling of the Charpy transition curve, Eng. Fract. Mech. 72 (2005) 413–434.
[4] C.M. Wang, J.D. Splett, Uncertainty in reference values for the Charpy V-notch verification program, J. Test. Eval. 34 (2005) 1–4.
[5] M. Ando, N.A. Noda, Y. Kuroshima, Y. Ishikawa, Impact properties of polydimethylsiloxane copolymerized polycarbonate and application of the time-temperature superposition principle, Trans. Jpn. Soc. Mech. Eng. 80 (2014) 149 (in Japanese).
[6] N.A. Noda, H. Ohtsuka, H. Zheng, Y. Sano, M. Ando, T. Shinozaki, W. Guan, Strain rate concentration and dynamic stress concentration for double-edge-notched specimens subjected to high-speed tensile loads, Fatigue Fract. Eng. Mater. Struct. 38 (2015) 125–138.
[7] P.E. Bennett, G.M. Sinclair, Parameter representation of low-temperature yield behavior of body-centered cubic transition metals, J. Basic Eng. 88 (1966) 518.
[8] E. Fujii, I. Ohkuma, Y. Kawaguchi, M. Tsukamoto, Effects of temperature and strain rate on dynamic fracture toughness of steel, J. Soc. Nav. Archit. Jpn. 158 (1985) 619–629 (in Japanese).
[9] T. Ikeda, T. Umetani, N. Kai, K. Ogi, N.A. Noda, Y. Sano, Influence of silicon content, strain rate and temperature on toughness and strength of solid solution strengthened ferritic ductile cast iron, Mater. Trans. 57 (2016) 2132–2138 (in Japanese).
[10] F. Minami, T. Hashida, M. Toyoda, J. Morikawa, T. Ohmura, K. Arimochi, N. Konda, Dynamic fracture toughness evaluation of structural steels based on the local approach, J. Soc. Nav. Archit. Jpn. 84 (1998) 453–464 (in Japanese).
[11] H. Yamamoto, T. Kobayashi, H. Fujita, Strain rate dependency of ductile-brittle transition behavior in ductile cast iron, J. Jpn. Foundry Eng. Soc. 72 (2000) 107–112 (in Japanese).
[12] H. Yamamoto, T. Kobayashi, H. Fujita, Strain rate-temperature dependency of impact tensile properties and ductile fracture behavior in ductile cast iron, Tetsu-to-Hagane 85 (1999) 765–770 (in Japanese).

[13] K. Gotoh, H. Hirasawa, M. Toyosada, A simple estimating method of constitutive equation for structural steel as a function of strain rate and temperature, J. Soc. Nav. Archit. Jpn. 176 (1994) 501–507.
[14] F. Minami, T. Hashida, M. Toyoda, J. Morikawa, T. Ohmura, K. Arimochi, N. Konda, Dynamic fracture toughness evaluation of structural steels based on the local approach, J. Soc. Nav. Archit. Jpn. 184 (1998) 453–464.
[15] H. Yamamoto, T. Kobayashi, H. Fujita, Strain rate-temperature dependency of impact tensile properties and ductile fracture behavior in ductile cast iron, Tetsu-to-Hagane 85 (1999) 765–770.
[16] N.A. Noda, Y. Takase, Fatigue Notch Strength Useful for Machine Design, Nikkan Kogyo Shimbun Ltd., Tokyo, 2010 (in Japanese).
[17] N.A. Noda, Y. Takase, Stress concentration factor formulas useful for all notch shapes in a flat test specimen under tension and bending, J. Test. Eval. 30 (2002) 369–381.
[18] N.A. Noda, Y. Takase, Generalized stress intensity factors of V-shaped notch in a round bar under torsion, tension, and bending, Eng. Fract. Mech. 70 (2003) 1447–1466.
[19] H. Nisitani, N.A. Noda, Stress concentration of a cylindrical bar with a V-shaped circumferential groove under torsion, tension or bending, Eng. Fract. Mech. 20 (1984) 743–766.
[20] N.A. Noda, Y. Takase, Stress concentration formula useful for all notch shape in a round bar (comparison between torsion, tension and bending), Int. J. Fatigue 28 (2006) 151–163.
[21] N.A. Noda, Y. Takase, K. Monda, Stress concentration factors for shoulder fillets in round and flat bars under various loads, Int. J. Fatigue 19 (1997) 75–84.
[22] M. Naitoh, M. Daimaruya, On the dynamic yield of metallic materials under impact loading, Trans. Jpn. Soc. Mech. Eng. 33 (1984) 801–807 (in Japanese).
[23] T. Ikeda, T. Umetani, N. Kai, K. Ogi, N.-A. Noda, Y. Sano, Strain rate and temperature insensitiveness of notch-bend strength for high Si ductile cast iron, ISIJ Int. 56 (2016) 868–874.
[24] T. Ikeda, T. Umetani, N. Kai, K. Ogi, N.-A. Noda, Y. Sano, Influence of silicon content, strain rate and temperature on toughness and strength of solid solution strengthened ferritic ductile cast iron, Mater. Trans. 57 (2016) 2132–2138.
[25] E. Fujii, I. Ohkuma, Y. Kawaguchi, M. Tsukamoto, Effects of Temperature and strain rate on dynamic fracture toughness of steel, J. Soc. Nav. Archit. Jpn. 158 (1985) 619–629.
[26] K. Gotoh, H. Hirasawa, M. Toyosada, A simple estimating method of constitutive equation for structural steel as a function of strain rate and temperature, J. Soc. Nav. Archit. Jpn. (1994) 501–507.